Oxygen vacancies in BaTiO$_3$

R. Scharfschwerdt, A. Mazur, O. F. Schirmer, H. Hesse, and S. Mendricks

Fachbereich Physik, Universität Osnabrück, D-49069 Osnabrück, Germany

(Received 24 June 1996)

Using electron paramagnetic resonance two types of Ti^{3+}-related centers are identified in BaTiO$_3$, which are attributed to Ti^{3+}-V_O and to Ti^{3+}-V_O associated with Na or K, respectively. This assignment is based on the chemical and illumination conditions leading to the detection of the defects. It is furthermore supported by the Ti hyperfine structure, resolved for Ti^{3+}-V_O-Na(K). The symmetry of the centers is broken in the sense that an electron is localized near one of the two equivalent Ti^{4+} ions next to V_O. Also the observed Ti hyperfine structure points to electron capture at one Ti site. The V_O-type centers are contrasted to isolated Ti^{3+}, representing a free small polaron in crystals containing Nb^{5+} and no oxygen vacancies. The participation of the V_O centers in photochromic processes in BaTiO$_3$ is studied. In crystals doped with Na or K an optical absorption precursor of the fundamental absorption is identified and attributed to the creation of an exciton bound to the V_O-Na(K) complex. [S0163-1829(96)08645-6]

I. INTRODUCTION

The role of oxygen vacancies V_O in oxide perovskites and especially in BaTiO$_3$ has been discussed extensively in the past. The question of whether the conductivity and near-infrared optical absorption in n-type BaTiO$_3$ is caused by oxygen vacancies or by free polarons has been investigated by numerous researchers (Berglund and Braun,[1] Berglund and Baer,[2] Bursian *et al.*,[3] Gerthsen *et al.*,[4] and Ihrig[5]). Smyth[6] reported that the presence of V_O in BaTiO$_3$ is strongly determined by the acceptor A' concentration. Unless the material is annealed under elevated oxygen pressures, the negatively charged A' are compensated by oxygen vacancies $(V_O)^{\bullet\bullet}$. Additional V_O can be created by reduction. The electrons left behind, if neutral oxygen leaves the crystal, are shared with the V_O initially present before reduction. All phenomena, especially the dependence of the electric conductivity on oxygen partial pressure, can be explained[6] if it is assumed that V_O is present in its fully ionized state $(V_O)^{\bullet\bullet}$ at T > 600 °C. This is supported by the low ionization energy of $(V_O)^{\bullet}$, 0.12 eV, as determined by Lewis and Catlow[7] via shell model calculations. Daniels and Härdtl,[8] on the other hand, postulated that complete ionization of V_O occurred only at higher temperatures. Little is known so far about the electronic and geometrical structure of V_O. In this context, Prosandeyev and Osipenko[9] and Donnerberg[10] have recently proposed that an electron captured at $(V_O)^{\bullet\bullet}$ is localized at one of the two equivalent cation neighbors of V_O in oxide perovskites, in this way breaking the symmetry of the oxygen site in such a crystal.

Most previous knowledge about V_O in BaTiO$_3$ results from theoretical arguments or from phenomenological experimental studies, i.e., investigations not taking recourse to the identification of the defects actually present in the crystals and to their submicroscopic models. In this paper we shall report on the electron paramagnetic resonance (EPR) of V_O in BaTiO$_3$, leading to the geometrical and electronic structures of this defect and the centers derived from it. A short account of some of the results has been published previously.[11] Using this information it will be possible to base additional phenomenological studies on well-established atomic-scale entities. This investigation is thus a step towards a complete understanding of the properties of the anion vacancies in this material, a situation having been established long ago for, e.g., the alkali halides[12] and the alkaline earth oxides.[13] It is expected that the experiences gathered with V_O in BaTiO$_3$ will be sample cases also for other oxide perovskites.

Because of the dependence of the V_O concentration on the acceptor content of the material, it is useful to compare the defect structure of BaTiO$_3$ crystals with enhanced as well as with deriched acceptor concentrations. In the latter case V_O will essentially only appear after a reduction treatment. Among the acceptors generally leading to the presence of compensating V_O, the alkali ions, replacing Ba, are an important subgroup. They are detected by the paramagnetism of an O$^-$ ion next to an alkali defect, formed after suitable illumination by capture of light induced holes. Recently we have published an extended overview on these defects.[14]

Only the charge state $(V_O)^{\bullet}$ is paramagnetic. Its EPR consists of Ti^{3+} signals, resulting from an electron captured at one of the two Ti^{4+} ions neighboring the oxygen vacancy. Ti^{3+} spectra of similar, but clearly different structure arise[15] in BaTiO$_3$ from quasifree conduction electrons, self-trapped as small polarons, i.e., as Ti^{3+} electrons surrounded by six O^{2-} ions instead of the five being present for (Ti^{3+}-V_O). Such quasifree electrons can be produced in acceptor deriched crystals, if these contain Nb^{5+} donors, compensated by Ti^{3+}. Here the electron is self-trapped, essentially by a $T_2 \times e$ Jahn-Teller effect,[15] causing a self-induced axiality. In most cases the polaron is not associated with Nb.[15] A comparison with such free small polarons is certainly also advisable in order to shed light on the specific properties of the oxygen vacancies. It will be discussed below how such centers can be discriminated from the V_O defects.

EPR spectra similar to those reported in this paper have been presented previously by Takeda and Watanabe[16] and by Zitková *et al.*;[17] they were attributed to axial V_O centers.
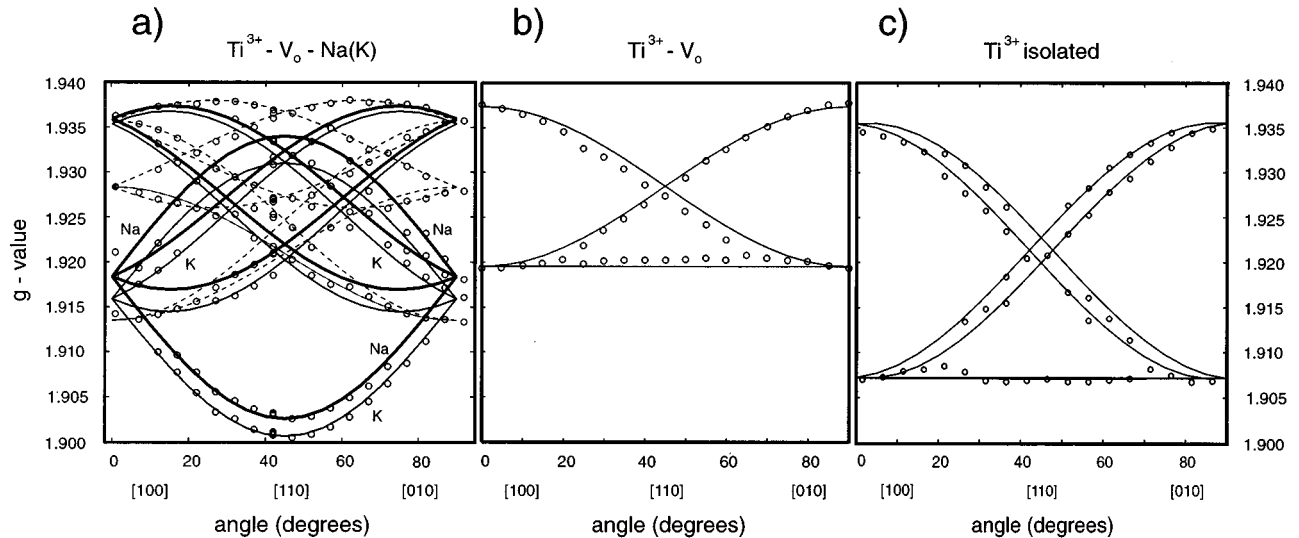
FIG. 1. Dependence of the g values for a variation of the magnetic field in a $\{001\}$-type plane. (a) Ti^{3+}-V_O-Na(K), (b) Ti^{3+}-V_O, and (c) isolated Ti^{3+}. In the latter case a slight tilting of the center axes, caused by the influence of the rhombohedral crystal field, was resolved. Such influences were not detected for the other two centers.

Even taking account of the rather large limits of error given by these authors,[17] their values of $g_\|$, however, are clearly lower than those determined by us. From the comparison of the chemical, optical, and electronic properties of the various Ti^{3+}-related defects which we identified we shall deduce that the assignment of our spectra to V_O centers is consistent with all observations.

We shall start by presenting the experimental details leading to the EPR results. In order to obtain a reliable foundation for the following additional experiments and their interpretation, the EPR data will be discussed first. Then further experimental evidence, as related to the charge change of the V_O centers by illumination and the stability of the $(V_O)^\bullet$ state will be given. A joint discussion of the data will conclude the paper.

II. EXPERIMENTAL DETAILS AND EPR-RELATED RESULTS

Multidomain crystals of typical size $1 \times 2 \times 3$ mm^3 were used. They had been grown from a TiO_2-enriched $BaTiO_3$ melt by the top seeded solution growth (TSSG) method in the crystal growth laboratory at the University of Osnabrück. Three types of specimens, pulled from the following melts, were investigated: (1) $BaTiO_3$ having an enhanced acceptor concentration (800 ppm Na or 1000 ppm K). The as-grown crystals of this type looked clear and transparent. (2) Pure $BaTiO_3$, derived from acceptors, especially from alkali ions and from donors (such as, e.g., Nb). Those crystals were water clear. (3) Acceptor-derided $BaTiO_3$, containing traces of Nb; this element was introduced as a background impurity with the starting material. Such crystals were bluish.

ESR spectra were taken at temperatures between 10 and 80 K with a Bruker 200 D SRC X-band spectrometer. At these temperatures $BaTiO_3$ has the structure of the rhombohedral phase. Since there are only very slight deviations from

cubic symmetry in this phase, the structure can be considered to have the latter symmetry for most practical purposes. Reducing treatments of the samples were performed at 850 °C in 10^5 Pa flowing H_2 gas. The specimens were cooled fast (within 30 s) to 450 °C after treatment.

Figure 1(a) shows the angular dependence of the resonance fields of the signals, assigned below to Ti^{3+}, observed at low temperatures with crystals of type 1 in their "as-grown" state after illumination with light of energies higher than 2.5 eV. Clearly the responsible defects have only orthorhombic or lower symmetry. The branches designated by K or Na were especially strong in spectra taken with crystals enriched with the respective ions. These crystals also led to a
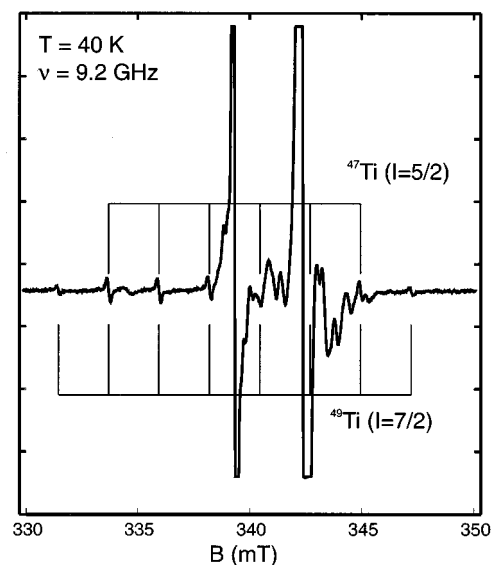

FIG. 2. ^{47,49}Ti hyperfine structure, bracketing the ESR of the $I=0$ isotopes of Ti.

TABLE I. g-tensor principal values and internal energy levels of defects in $BaTiO_3$ containing Ti^{3+}.

	Axial centers	$g_\parallel$	$g_\perp$	$g_\perp$	τ	$E_\parallel$	$E_\perp$	Ref.
						$(10^4$ cm$^{-1})$	
1	Free small polaron	1.934(2)	1.907(2)	1.907(2)	4(1) [a]	1.81(5)	0.323(6)	15
2	V_O center	1.937(1)	1.920(1)	1.920(1)	0	1.89(3)	0.374(4)	this paper
3	V_O-related center	1.930	1.911	1.911	0	1.70	0.337	16
4	V_O-related center	1.930(4)	1.916(6)	1.916(6)	0	1.70(8)	0.36(2)	17
	Nonaxial centers							
	(a) (110) mirror plane	$g_{[001]+\tau}$	$g_{[110]}$	$g_{[1\bar{1}0]+\tau}$				
5	V_O associated with K	1.937(1)	1.931(1)	1.899(1)	12(1)	1.89(3)	0.365(4) [b]	11
6	V_O associated with Na	1.938(1)	1.934(1)	1.901(1)	12(1)	1.91(3)	0.378(4) [b]	11
	(b) (100) mirror plane	$g_{[001]+\tau}$	$g_{[010]}$	$g_{[100]+\tau}$				
7	V_O associated with acceptor on Ti site?	1.938(1)	1.926(1)	1.914(1)	26(2)	1.91(3)	0.376(4) [b]	this paper

[a]Small deviation from axial symmetry by influence of rhombohedral crystal field resolved for this center.
[b]Mean value of two lowest-energy splittings indicated. All energy values are based on $\lambda_{Ti} = 154$ cm^{-1}.

second type of Ti^{3+} related resonances of low symmetry; the representative branches are indicated by dashes in Fig. 1(a). As-grown specimens of type 2 showed very little Ti^{3+} related spectra under the same illumination conditions. Much larger signals, now related to axial symmetry [Fig. 1(b)] of the underlying centers, were observed after reduction treatment, and no additional illumination was then necessary. For comparison, also the axial angular dependence of isolated Ti^{3+} small polarons, identified in crystals of type 3, is shown [Fig. 1(c)]. They too are observed without prior illumination. Table I lists the principal values and the directions of the principal axes of the g tensor of all the observed Ti^{3+}-related resonances.

For the low-symmetry centers observed with crystals of type 1, the hyperfine interaction caused by the Ti isotopes with magnetic nuclei (^{47}Ti, $I = 5/2$, $g_n = -0.3154$, 7.4%;
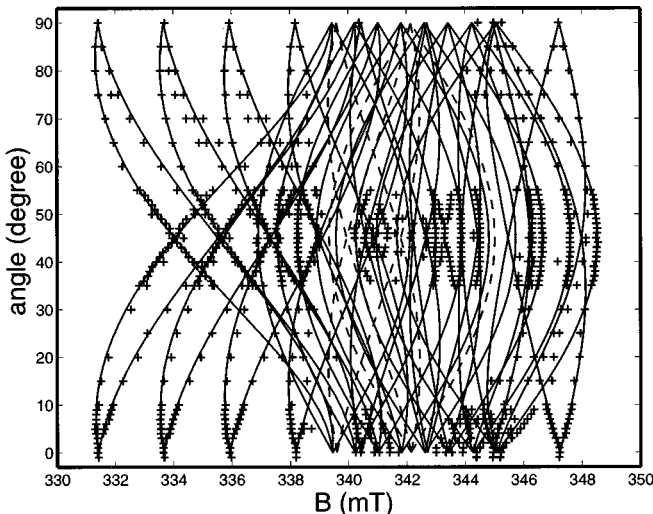
^{49}Ti, $I = 7/2$, $g_n = -0.3155$, 5.4%) was resolved (Fig. 2). Since both values of g_n differ by less than 10^{-3}, the hyperfine pattern of ^{47}Ti coincides with that of ^{49}Ti. Of the latter only the outer lines ($m_I = \pm 7/2$) stand isolated. The dependence of the Ti hyperfine structure on the direction of the magnetic field (Fig. 3) can be described by the hyperfine tensor given in Table II. In evaluating this data, use has been made of the program package 'R−spectr.'[18]

III. DISCUSSION OF EPR RESULTS

The hyperfine structure proves the presence of Ti, whereas the g-tensor components identify the charge state of Ti as Ti^{3+}; see Ref. 19. The spectra can be reproduced with the Hamiltonian $\mathcal{H} = \mu_B \boldsymbol{BgS} + \boldsymbol{IAS} + g_n \mu_B \boldsymbol{BI}$ with $S = 1/2$ and $I = 5/2$ or $I = 7/2$. The lines in Figs. 1(a), 1(b), and 1(c) are fits to the experimental line positions, leading to the entries in Table I. As far as the hyperfine interaction could be resolved, it is consistent with the data in Table II. Models taking into account all the experimental information are presented in Figs. 4(a), 4(b), and 4(c).

The following facts point to association of V_O with Ti^{3+} as the responsible defects: Crystals of type 1, containing alkali acceptors,[14] which are known to be compensated by V_O, show the Ti^{3+} resonances (see Fig. 1 and Table I), centers 5 and 6, after near band-gap illumination. The dependence of the spectra on the Na or K content, in the case of type-1 crystals, leads to assume that the electron, forming

FIG. 3. Angular dependence of the ^{47,49}Ti hyperfine structure. The line position of the $I = 0$ isotopes are shown dashed.

TABLE II. Ti hyperfine tensor principal values. Hyperfine interaction resolved for Ti^{3+}-V_O-Na(K) only. Energy values in 10^{-4} cm^{-1}. Within the limits of error, the hyperfine parameters are identical for ^{47}Ti and ^{49}Ti. The signs of the hyperfine tensor components cannot be deduced from the experimental data.

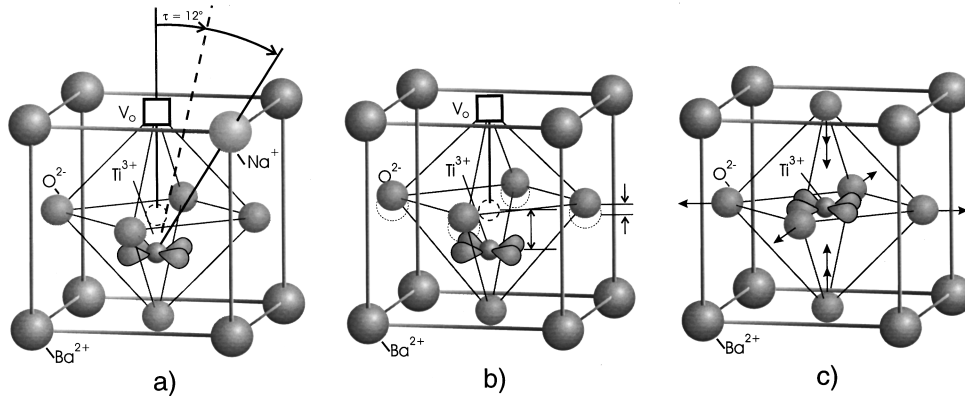| $|A_{[001]+\tau}|$	$|A_{[110]}|$	$|A_{[1\bar{1}0]+\tau}|$	τ
20.41	6.14	8.13	5°

FIG. 4. Models derived from the data in Fig. 1. (a) Ti^{3+}-V_O-Na(K), (b) Ti^{3+}-V_O, and (c) isolated Ti^{3+}.

Ti^{3+}, is captured close to a V_O-alkali complex [Fig. 2(a)]. The presence of an alkali ion in the center also explains why the symmetry is lower than axial. It is only C_s; the {110} mirror plane, shown in Fig. 5, contains Ti^{3+}, V_O, and Na (or K). The observed tilting of the g-tensor axes by 12° occurs in such planes. The other low-symmetry Ti^{3+} defects, center 7 in Table I, have {100}-type mirror planes. No definite assignment is possible so far. Probably a Ti^{3+}-V_O pair associated with an acceptor on a Ti site is involved.

An axial configuration C_{4v} (center 2 in Table I) is observed in alkali-deriched crystals (type 2) after reduction and without illumination. Evidently, a reducing treatment is necessary to introduce these defects, since there are no acceptors requiring V_O for compensation. After reduction the Fermi level apparently lies at $(V_O)^{••/•}$ or at $(V_O)^{•/x}$ (Fig. 6), because the EPR of $(V_O)^{•}$ is here observed without additional illumination. Figure 4(b) exhibits the model of the resulting centers. Crystals of type 3, containing isolated Ti^{3+} [see Fig. 4(c) and Table I, center 1], show the related resonances without prior illumination or reduction treatment, because the Nb traces in such specimens are compensated by Ti^{3+}.

It should be noted that the tilting angle of the V_O-alkali centers, 5 and 6 in Table I, would be zero, if the electron was shared between the two Ti^{4+} ions below and above V_O in Fig. 5. Evidently the symmetry resulting from the equivalence of the two Ti^{4+} ions neighboring V_O is broken. The same conclusion is drawn from the Ti hyperfine interaction: If two Ti were equally coupled, 11
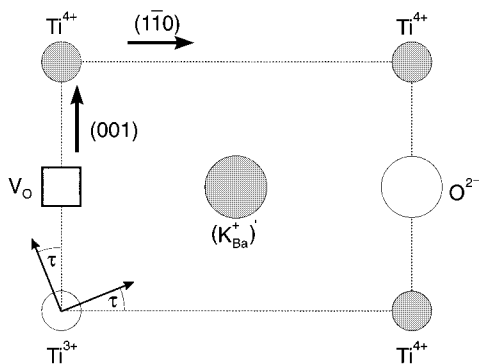
lines would be expected for ^{47}Ti having the intensities 1 : 2 : 3 : 4 : 5 : 6 : 5 : 4 : 3 : 2 : 1, and correspondingly for ^{49}Ti. The observed number of hyperfine lines (Fig. 2) and their intensities relative to the large lines resulting from ($I=0$) isotopes point to interaction with one Ti nucleus. One expects that the influence of the alkali partner, midway between both possible Ti positions, on the localization of the Ti^{3+} electron is weak, since the distance between Na (or K) and Ti^{3+} is rather large compared to Ti^{3+}-V_O (Fig. 5). Therefore it is likely that this symmetry breaking also prevails in the axial, alkali-free centers. In this case EPR cannot decide whether the electron is localized at one Ti site (broken symmetry) or shared between two (full symmetry), because the symmetry is axial around the Ti^{3+}-V_O axis in both situations. (Unfortunately, hyperfine interaction could not yet be resolved for the axial Ti^{3+}-V_O centers.) We are thus led to assume that V_O centers in the oxide perovskites show broken symmetry in the sense that one of the equivalent Ti^{4+} ions is singled out by electron capture. This supports the relevant prediction made by Prosandeyev and Osipenko.[9] Such symmetry breaking occurs also for the antimorphs of the $(V_O)^{•}$ centers in oxide materials, i.e., for cation vacancies, when holes are captured at one of the O^{2-} next to them,[20] and also for other acceptor dopings.[21,14] On the other hand, electron capture near sixfold-coordinated V_O, e.g., $(V_O)^{•}$ in MgO or CaO, does not break the cubic symmetry.[13] Neither is the symmetry broken in the familiar F centers in alkali halides.[12]

Considering the shifts Δg_i between the measured g-tensor components in Table I and g_e, the value of the free electron, we shall now demonstrate the following: (1) The energy levels of axial (center 2 in Table I) and low-symmetry centers (5, 6, and 7 in Table I) are nearly identical, as expected on account of the proposed models. (2) The levels of these centers are different from those of the isolated Ti^{3+}
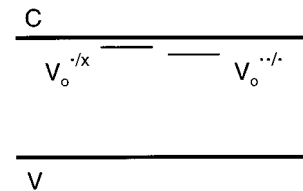

FIG. 5. The mirror plane of Ti^{3+}-V_O-Na(K).

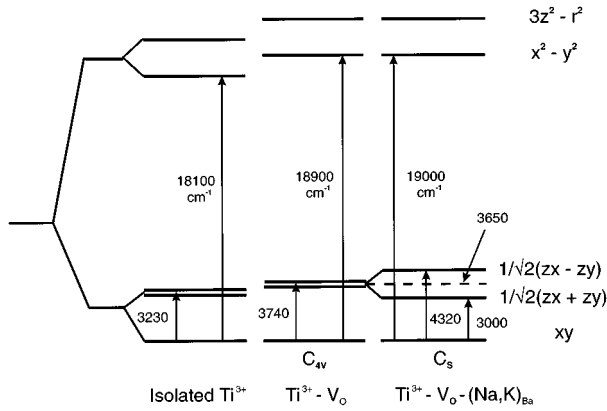
FIG. 6. The two energy levels expected for V_O centers.

FIG. 7. Energy levels of the Ti^{3+}-related centers; see also Table I. The EPR results do not depend on the energy of the $(3z^2-r^2)$ level. It is possible that this lies much lower than indicated.

FIG. 8. Optical transition leading from an alkali acceptor to a nearby Ti^{4+}-V_O, creating an exciton bound to the complex shown in Fig. 5.

small polaron (center 1). (3) The levels of centers 3 and 4, reported by Takeda and Watanabe[16] and by Zitková *et al.*,[17] differ from those presented here.

The ground-state T_2 orbital triplet of Ti^{3+} in cubic symmetry is split by the V_O axial field in such a way that an orbital singlet lies lowest (Fig. 7). Otherwise, the orbital angular momentum would not be quenched, and the values of g_i would strongly differ from g_e. The sequence $\Delta g_\parallel > \Delta g_\perp$ points to an xy ground state. For this situation the Δg_i are given by[22] $\Delta g_\parallel = -8\lambda/E_\parallel$ and $\Delta g_\perp = -2\lambda/E_\perp$, where λ is the spin-orbit coupling constant of the free Ti^{3+} ion, 154 cm^{-1}. The corresponding value might be different for Ti^{3+} in its crystalline environment. But since we are interested only in the relationships of the energy denominators $E_\parallel$ and $E_\perp$ in the different centers, we shall adopt the above value and find then the energy distances indicated in Fig. 7 and listed in Table I. For the low-symmetry V_O centers, the expression for $\Delta g_\parallel$ is not changed, whereas $\Delta g_\perp$ is replaced by $\Delta g_1 = -2\lambda/E_1$ for the $B\parallel$ mirror plane and $\Delta g_2 = -2\lambda/E_2$ for the $B\perp$ mirror plane. For these low-symmetry centers the mean values of E_1 and E_2 are listed in Table I. (1) It is seen that the energies $E_\perp$, about 0.37×10^4 cm^{-1} for the axial defect (center 2) and also for the nonaxial ones (centers 5, 6, and 7), are nearly identical within the limits of error. Also, the high energies $E_\parallel$, about 1.90×10^4 cm^{-1}, coincide. This supports the close relationship between these centers and assigns them, on the basis of the previous arguments, to variants of the oxygen vacancy. (2) The respective energy values for isolated Ti^{3+} (center 1), the free small polaron, are 0.323×10^4 cm^{-1} and 1.81×10^4 cm^{-1}, distinctly lower than for the V_O centers. This is evidence that indeed another structure is present. (3) The level energies of centers 3 and 4, attributed in Refs. 16 and 17 to oxygen vacancies, are different from those identified here for V_O-related defects: Even taking account of the large limits of error, listed only in the work of Zitková *et al.*,[17] it is seen that especially the $E_\parallel$ energies of centers 3 and 4, which are $\sim 1.70 \times 10^4$ cm^{-1}, are smaller than those of the V_O centers (2, 5, 6, and 7), which are $\sim 1.9 \times 10^4$ cm^{-1}. The structure of the centers 3 and 4 is unknown so far. It should be noted, however, that both of these were observed[16,17] with $BaTiO_3$ crystals grown
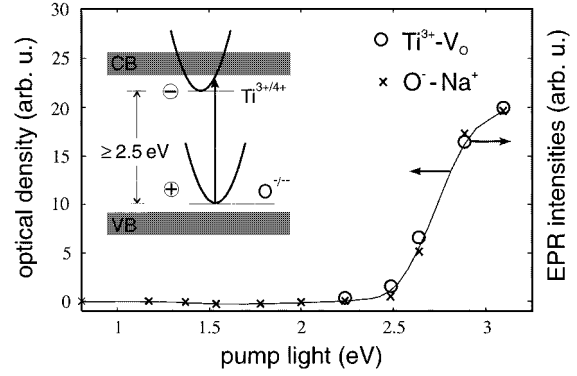
from KF flux, whereas in our case a pure $BaTiO_3$ melt, enriched in TiO_2, and Czochralski growth was used. Müller *et al.*[23] attribute these centers to an axial Ti^{3+} V_O, further associated with an acceptor ion on a Ti position at the other side of V_O in Fig. 3. The angular dependence of centers 5 and 6 turns out to be qualitatively similar to the behavior of spectra also reported by Takeda and Watanabe.[16] No assignment was given for these signals by the authors.

For the axial V_O Ti^{3+} center the ratio of the two energies listed above has been used to derive information on the lattice distortion around Ti^{3+}. This ratio is independent of the reduction of the spin-orbit coupling, occurring if Ti^{3+} is incorporated in its crystalline surroundings. In the evaluation it has been assumed that movements of the indicated ions take place only along the axis of the shown model. On the basis of a point ion crystal field calculation, adopting the Hartree-Fock values $\langle r^2 \rangle = 1.89$ a.u. and $\langle r^4 \rangle = 7.07$ a.u. (Ref. 24) for the Ti^{3+} d orbital, one derives the distortion scheme presented in Fig. 4(b). It is seen that the Ti^{3+} ion relaxes away from V_O by 0.35 Å, into the cage of the remaining five O^{2-} ions. A countermovement of the four equatorial O^{2-} ions by 0.11 Å supports this tendency. This relaxation around Ti^{3+} is expected because it increases the chemical binding of Ti^{3+} to its neighbors. Of course it should be considered that the derived distances are rather crude estimates.

The Ti hyperfine interaction is nearly axially symmetric around a direction tilted by 5° in the same sense [see Fig. 4(a)] as the corresponding g-tensor principal axis. Adopting an axial approximation we have $A_\perp = 7.13 \times 10^{-4}$ cm^{-1} and $A_\parallel = 20.41 \times 10^{-4}$ cm^{-1} from Table II. For an xy ground state we have the relations[24] $A_\parallel = a + P(\Delta g_\parallel - 4/7), A_\perp = a + P(\Delta g_\perp + 2/7)$, where $P = (\mu_0/4\pi)g_e\mu_B g_i\mu_k\langle r^{-3}\rangle$ and $a = (2/3)(\mu_0/4\pi)g_e\mu_B g_i\mu_k|\psi(0)|^2$, the contact interaction. Evaluating the data in Table II under the assumption that all hyperfine tensor components have negative sign, we find $P = 15.8 \times 10^{-4}$ cm^{-1} and $a = -10.3 \times 10^{-4}$ cm^{-1}. The value of P corresponds to $\langle r^{-3}\rangle = 1.6$ a.u., 63% of the free ion value $\langle r^{-3}\rangle = 2.55$ a.u.[24] This reduction is certainly caused by the larger delocalisation of the Ti^{3+} valence electron in the crystal. Another possible choice of signs, $A_\parallel < 0, A_\perp > 0$, predicts $\langle r^{-3}\rangle = 3.2$ a.u., a physically unreal-

istic value, since it is larger than the free ion value. Neither is the adoption of the opposite signs for $A_\parallel$ and $A_\perp$ a reasonable choice; while still reproducing the experimental spectra, such values lead to $a > 0$, inconsistent with the core polarization origin of the hyperfine interaction of d orbitals.

Axial Ti^{3+}-V_O centers are not observed after reduction of alkali containing crystals, although new V_O, expected to be isolated, are produced by this treatment. This is proved by the observation that the EPR of the alkali-associated Ti^{3+}-V_O is now observed without illumination. Apparently the Fermi level E_F has been raised by a reduction in such a way that E_F lies at $(V_O)^\bullet$. A recent embedded cluster modeling[25] of $(V_O$-Ti$^{3+})$ and $(V_O$-Ti^{3+}-Na) indicates that an electron is trapped more stably at the latter species. This might explain why in this case no axial (Ti^{3+}-V_O) is found.

Finally, additional arguments supporting the discrimination between the isolated Ti^{3+} polaron and Ti^{3+} associated with V_O are forwarded: The observability of isolated Ti^{3+} requires neither reduction nor illumination, consistent with the fact that here Ti^{3+} is present as a compensator of the Nb^{5+} donor. As expected, the concentration of the Ti^{3+} polaron is also not decreased by oxidation. Furthermore, the response of both centers to uniaxial stress is different: While the axis of isolated Ti^{3+} aligns itself along the direction of [100] stress, P, already for $P < 5 \times 10^7$ Pa, Ti^{3+}-V_O shows no such response. This softness of isolated Ti^{3+} results from the fact that here an electronic rearrangement takes place: Stress favors an xy-orbital ground state, corresponding to a prolate symmetry of the center and its surroundings. Thus a rearrangement of electrons initially in other orbitals, zx or zy, to xy takes place. In the (Ti^{3+}-V_O) centers an ionic reorientation would have to occur.

IV. LIGHT-INDUCED RECHARGING OF V_O CENTERS

The illumination of acceptor containing crystals with light of energy $E > 2.5$ eV populates Ti^{3+}-V_O-type centers, as just mentioned, but also O$^-$ holes trapped near alkali acceptors are formed at low temperatures.[14] The dependence of the creation efficiencies of both species on light energy are parallel to each other (Fig. 8). This observation could be attributed to valence band electrons being excited to V_O-type centers. The holes created in this way can subsequently be trapped near acceptor sites. However, the rise of paramagnetism at 2.5 eV, already 0.7 eV below the band gap, is inconsistent with the trap level of V_O, being expected to be about 0.2 to 0.3 eV.[25] Also, the excitation of an electron from an O^{2-} ion next to an alkali acceptor to the conduction band, accompanied by subsequent trapping of the electron near V_O, will occur only at higher energies, since the respective acceptor level again is very shallow, about 0.05 eV.[14] An explanation of the difference between the threshold for the rise of paramagnetism and the band gap probably necessitates the assumption that the responsible electron excitation takes place from O^{2-} within a cluster as shown in Fig. 5 to the Ti^{3+} site. Then electron and hole attract each other, forming an exciton bound to the V_O-alkali complex. The exchange interaction between electron and hole is not observed, however, neither in the resulting O$^-$ nor in the (Ti^{3+}-V_O-Na) EPR spectra. Both can be described by isolated $S = 1/2$ entities. This might be caused by the large dis-

tance between Ti^{3+} and O$^-$, 0.6 nm (Fig. 3).

Although illumination is not necessary to create the paramagnetic (Ti^{3+}-V_O) in reduced crystals, grown from a melt deriched of alkali ions, the concentration of $(V_O)^\bullet$ is again enhanced in such material by illumination. As a result, also O$^-$-type centers are observed. These, however, have a lower concentration and consist mainly in a so-far unidentified species, probably containing Pt in an unknown charge state.[14]

V. CONCLUSION

We have identified the structure of Ti^{3+}-V_O-type centers in BaTiO$_3$ and compared it to that of the isolated Ti^{3+} small polaron. Although both types of centers have axial or nearly axial symmetry, they show distinctly different properties: unlike internal excitation energies, a changed behavior under illumination and redox treatment and different responses to uniaxial stress. Whereas the Ti^{3+}-V_O-Na(K) variant of the oxygen vacancy is a rather stable defect, observed in many crystals, the simple center, Ti^{3+}-V_O, is detected only after specifically reducing rather pure, especially acceptor-free crystals, and has the tendency to decay, if kept in normal atmosphere. This elusiveness may be caused by the following circumstances: Oxygen vacancies have the tendency to associate with the Na and K acceptors, which are frequently met in BaTiO$_3$ crystals. In specimens containing transition metal acceptors, also associations with such defects are known to form, such as Fe^{3+}-V_O. For an overview see Ref. 26. If Ti^{4+}-V_O and Ti^{4+}-V_O-Na(K) coexist in the same crystal, an added electron will have a lower energy at the latter defect, and Ti^{3+}-V_O will then not be observed.[25] Also, the (Ti^{3+}-V_O) center appears to incorporate oxygen with a lower reaction enthalpy than [Ti^{3+}-V_O-Na(K)].

Important additional properties of the V_O centers, such as their optical absorption and their energy levels with respect to the conduction band edge, could not yet be identified. In order to base these data on established atomic-scale structures, we plan to identify optical absorption bands and energy levels by measurements simultaneously performed with ESR.

Note added in proof. We remark that most recent embedded cluster calculations[25] have identified a $(3z^2 - r^2)$ orbital to be the ground state of isolated Ti^{3+} $-V_O$. Only if this defect is associated —axially or nonaxially—with an acceptor type defect, an (xy) type orbital is predicted to be lowest. Therefore, the axial centers labelled Ti^{3+} $-V_O$ in the present paper might still be adjacent to an unidentified acceptor ion.

[1] C. N. Berglund and H. S. Braun, Phys. Rev. **164**, 790 (1967).

[2] C. N. Berglund and W. S. Baer, Phys. Rev. **157**, 358 (1967).

[3] E. V. Bursian, Y. G. Girshberg, and E. N. Starov, Phys. Status Solid B **46**, 529 (1971).

[4] P. Gerthsen, R. Roth, K. H. Härdtl, and H. G. Reik, Solid State Commun. **3**, 165 (1965).

[5] H. Ihrig, Solid State Phys. **9**, 3469 (1975).

[6] D. M. Smyth, Prog. Solid State Chem. **15**, 145 (1984).

[7] G. V. Lewis and C. R. A. Catlow, J. Phys. Chem. Solids **47**, 89 (1986).

[8] J. Daniels and K. H. Härdtl, Philips Res. Rep. **31**, 489 (1976).

[9] S. A. Prosandeyev and I. A. Osipenko, Phys. Status Solidi B **192**, 37 (1995).

[10] H. Donnerberg, Phys. Rev. B **50**, 9053 (1994).

[11] R. Scharfschwerdt, O. F. Schirmer, H. Kröse, and T. Kool, Ferroelectrics **185**, 9 (1996).

[12] W. B. Fowler, *Physics of Color Centers* (Academic, New York, 1968).

[13] B. Henderson and J. E. Wertz, *Electron Spin Resonance: Elementary Theory and Practical Applications* (Taylor & Francis, London, 1977).

[14] T. Varnhorst *et al.*, Phys. Rev. B **53**, 116 (1996).

[15] E. Possenriede *et al.*, Ferroelectrics **151**, 199 (1994).

[16] T. Takeda and A. Watanabe, J. Phys. Soc. Jpn. **21**, 267 (1966).

[17] J. Zitková, K. Ždánský, and Z. Šroubek, Czech. J. Phys. B **17**, 636 (1967).

[18] V. G. Grachev, c/o Fachbereich Physik, University of Giessen, D-35392 Giessen.

[19] O. F. Schirmer and K. A. Müller, Phys. Rev. B **7**, 2986 (1973).

[20] J. E. Wertz, G. S. Saville, L. Hall, and P. Auzins, J. Phys. Soc. Jpn. Suppl. II **18**, 305 (1963).

[21] O. F. Schirmer, J. Phys. Chem. Solids **32**, 499 (1971).

[22] J. E. Wertz and J. R. Bolton, *Electron Spin Resonance* (McGraw-Hill, New York, 1972), p. 31.

[23] K. A. Müller, W. Berlinger, and R. S. Rubins, Phys. Rev. **186**, 361 (1969).

[24] A. Abragam and B. Bleaney, *Paramagnetic Resonance of Transition Ions* (Oxford University Press, Oxford, 1970).

[25] A. Birkholz and H. Donnerberg (unpublished).

[26] O. F. Schirmer, H.-J. Reyher, and M. Wöhlecke, in *Insulating Materials for Optoelectronics*, edited by F. Agulló-López (World Scientific, Singapore, 1995).